THE JOURNAL OF PHYSICAL CHEMISTRY LETTERS
A JOURNAL OF THE AMERICAN CHEMICAL SOCIETY

pubs.acs.org/JPCL

Letter

Generalized Resonance Energy Transfer Theory: Applications to Vibrational Energy Flow in Optical Cavities

Jianshu Cao*

Cite This: J. Phys. Chem. Lett. 2022, 13, 10943−10951

Read Online

ACCESS | Metrics & More | Article Recommendations | Supporting Information

ABSTRACT: A general rate theory for resonance energy transfer (gRET) is formulated to incorporate any degrees of freedom (e.g., rotation, vibration, exciton, and polariton) as well as coherently coupled composite donor or acceptor states. The compact rate expression allows us to establish useful relationships: (i) detailed balance condition when the donor and acceptor are at the same temperature; (ii) proportionality to the product of dipole correlation tensors, which is not necessarily equivalent to spectral overlap; (iii) scaling with the effective coherent size, i.e., the number of coherently coupled molecules or modes; (iv) decomposition of collective rate in homogeneous systems into the monomer and coherence contributions such that the ratio of the two defines the quantum enhancement factor F; (v) spatial and orientational dependences as derived from the interaction potential. For the special case of exciton transfer, the general rate formalism reduces to FRET or its multichromophoric extension. When applied to cavity-assisted vibrational energy transfer between molecules or within a molecule, the general rate expression provides an intuitive explanation of intriguing phenomena such as cooperativity, resonance, and nonlinearity in the collective vibrational strong coupling (VSC) regime, as demonstrated in recent simulations. The relevance of gRET to cavity-catalyzed reactions and intramolecular vibrational redistribution is discussed and will lead to further theoretical developments.

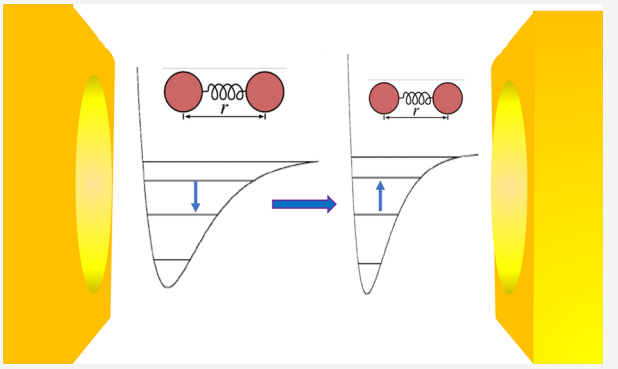

Energy transfer is a fundamental process in chemical physics and plays a pivotal role in photosynthesis, photovoltaics, and chemical dynamics in general. Much of our understanding is derived on the basis of a specific energy form, such as Forster resonance energy transfer (FRET) for excitons[1−3] and intermolecular or intramolecular energy relaxation for vibrations,[4,5] and is mostly limited to independent donors or acceptors. The first goal of this Letter is the formulation of a generalized resonant energy transfer (gRET) theory, which features two-fold generalizations: (i) applicability to any resonance quantum transfer processes including electronic, vibrational, and rotational transitions as well as hybrid energy transfer processes such as vibronic resonance and polariton resonance and (ii) extension from individual molecules to a collection of molecules coherently coupled via molecular interactions or optical cavity fields. As a special case, the rate formalism reduces to Forster resonance energy transfer (FRET) or its multichromophoric (MC) version for excitation energy transfer. The compact gRET rate expression allows us to establish its detailed balance (DB) condition, proportionality to the overlap of dipole correlation tensors, scalings with the effective coherent size, decomposition of the collective transfer rate in homogeneous systems, and configurational dependence.

The second goal of the Letter is the application of gRET to describe vibrational energy flow in optical cavities. As demonstrated in recent experiments,[6−12] the electromagnetic field of an optical cavity can mix with vibrational modes of molecular systems to collectively form vibrational polaritons and thus facilitate vibrational energy transfer (VET) between molecules or within a molecule and even modify chemical kinetics in the vibrational strong coupling (VSC) regime. These intriguing findings have stimulated theoretical and numerical studies, including molecular dynamics simulations of VET in cavities.[13−17] In particular, to develop a basic understanding of cavity-assisted VET, we apply the gRET rate expression to explain several observations reported in a recent cavity molecular dynamics simulation.[16]

Generalized RET Theory. The generalized resonance energy transfer (gRET) between a donor (D) and an acceptor (A) as illustrated by Figure 1a is described by the total Hamiltonian

$$H_{\text{total}} = H + H_{DA} = H_D + H_A + H_{DA}$$

Received: September 1, 2022
Accepted: November 9, 2022

https://doi.org/10.1021/acs.jpclett.2c02707
J. Phys. Chem. Lett. 2022, 13, 10943−10951

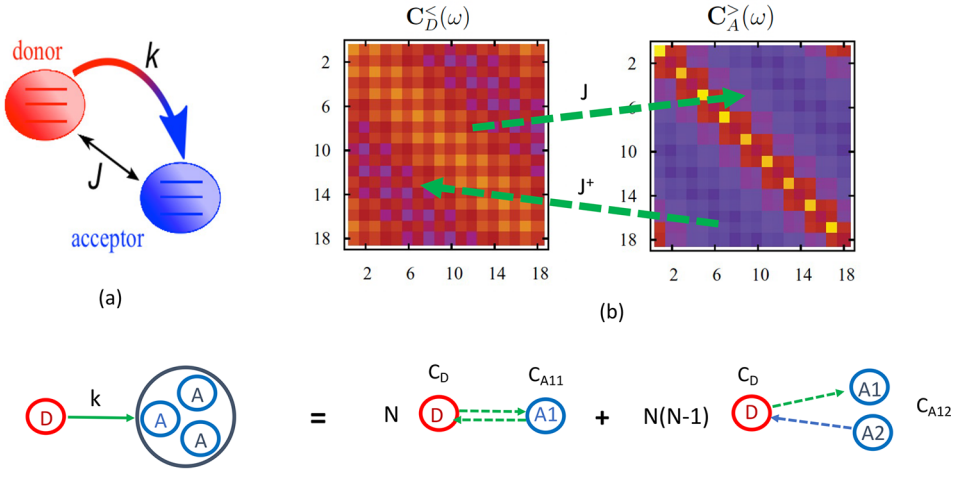

Figure 1. (a) Illustration of generalized resonance energy transfer (gRET); (b) gRET rate evaluated as the product of donor and acceptor dipolar correlation tensors mediated by the effective dipolar coupling tensor; (c) decomposition of coherence-enhanced rate in homogeneous systems to monomer contribution and coherence contributions, where the ratio of the two defines the quantum enhancement factor F.

where H_{DA} is the coupling between the donor and acceptor, $H_{A(D)}$ is the acceptor (donor) Hamiltonian, and $H = H_A + H_D$ is the uncoupled part of the total Hamiltonian. In a multichromophoric (MC) system, the donor or acceptor state can represent an aggregate of coherently coupled molecules and is therefore not limited to monomers. The interaction Hamiltonian between the donor and acceptor is given by

$$H_{DA} = \boldsymbol{\mu}_D^- \mathbf{J} \boldsymbol{\mu}_A^+ = \sum_{m=1}^{N_A} \sum_{n=1}^{N_D} \vec{\mu}_{D,m}^- \mathcal{J}_{mn} \vec{\mu}_{A,n}^+ \tag{1}$$

where $\mathcal{J}_{mn}$ depends on the intermolecular configuration and will be treated perturbatively. In eq 1, $\boldsymbol{\mu}^+$ and $\boldsymbol{\mu}^-$ represent the raising and lowering parts of the dipole operator, respectively. For N molecules in three-dimensional space, $\boldsymbol{\mu} = \{\vec{\mu}_n\}$ is the $3N$ dipole vector and $\mathbf{J} = \{\mathcal{J}_{mn}\}$ is the $(3N) \times (3N)$ coupling tensor. Hereafter, bold font represents vectors and tensors in the $3N$ dimensional space and the calligraphic font represents tensors in the three-dimensional space.

The acceptor (donor) Hamiltonian is a function of the molecular degrees of freedom as well as solvent, cavity, and all the other degrees of freedom associated with the acceptor (donor) state. For a vibrational degree of freedom, a compact notation to represent such a state is

$$|A\rangle = |\nu\rangle_A |b\rangle_A |c\rangle_A = |\nu_1, \cdots, \nu_n, \cdots\rangle_A |b\rangle_A |c\rangle_A$$

where ν_n is the vibrational quantum number of the nth molecule, b represents the set of bath modes, and c represents the cavity mode(s). The donor state $|D\rangle$ is defined similarly.

To formulate the gRET theory, we should understand the temporal and spatial scales involved in the resonance energy transfer process. (i) The rate process describes the incoherent transfer from a donor to an acceptor, which occurs after the donor is in equilibrium with its thermal bath and cavity field or in a nonequilibrium steady-state (NESS) under constant pumping. In other words, the donor or acceptor relaxes to a stationary state on a time scale much faster than the energy transfer time $1/k$. (ii) Spatially, the density matrix can be delocalized within the donor or acceptor manifold but not in between. If the molecules in the donor or acceptor manifolds are coherently coupled, the density matrix is delocalized and energy transfer exhibits cooperativity. In contrast, if quantum coherence is suppressed by static and dynamical disorder, then the density matrix is localized and energy transfer does not exhibit any cooperativity. The extent of the spatial localization, i.e., stationary quantum coherence, is quantified by N_{coh}, which determines the degree of cooperativity in energy transfer rate.

Based on the above conditions, the forward gRET rate can be obtained straightforwardly from Fermi's golden rule rate,[18] giving

$$k = \frac{2\pi}{Z_D} \sum_{\text{initial,final}} \rho_{\text{initial}} |\langle \Psi_{\text{final}} | H_{DA} | \Psi_{\text{initial}} \rangle|^2 \delta(E_{\text{final}} - E_{\text{initial}}) \tag{2}$$

where the subscripts *initial* and *final* refer to the initial and final states, respectively. Here, $|\Psi\rangle = |D\rangle\,|A\rangle$ is the composite donor−acceptor state and $E = E_A + E_D$ is the corresponding eigen-energy associated with the uncoupled Hamiltonian $H = H_A + H_D$. The initial state distribution function ρ_{initial} is diagonal in the eigenstate basis and can be factorized as $\rho_{\text{initial}} = \rho_A \rho_D$. $Z_D = \text{Tr}(\rho_D)$ is the donor partition function.

To proceed, we transform eq 2 to the time domain and obtain

$$\begin{aligned} Z_D k &= \int_{-\infty}^{\infty} \mathrm{d}t \,\text{Tr}[H_{DA}^+(t) H_{DA}(0) \rho_{\text{initial}}] \\ &= \int_{-\infty}^{\infty} \mathrm{d}t \,\text{Tr}[\boldsymbol{\mu}_D^-(0) \rho_D \boldsymbol{\mu}_D^+(t)] \mathbf{J} \,\text{Tr}[\boldsymbol{\mu}_A^-(t) \boldsymbol{\mu}_A^+(0) \rho_A] \mathbf{J}^+ \end{aligned}$$

where the trace is taken over all degrees of freedom and the time-dependence in operators arises from the interaction picture representation, $\boldsymbol{\mu}(t) = \exp(\mathrm{i}Ht)\boldsymbol{\mu}\exp(-\mathrm{i}Ht)$ and $H_{DA}(t) = \exp(\mathrm{i}Ht)\, H_{DA} \exp(-\mathrm{i}Ht)$. To simplify the rate expression, we introduce dipole correlation tensors as

$$\mathbf{C}^>(t) = \text{Tr}[\boldsymbol{\mu}^-(t)\boldsymbol{\mu}^+(0)\rho]$$

$$\mathbf{C}^<(t) = \text{Tr}[\boldsymbol{\mu}^+(0)\boldsymbol{\mu}^-(t)\rho]^{\mathrm{T}} = \text{Tr}[\boldsymbol{\mu}^-(t)\rho\boldsymbol{\mu}^+(0)]$$

and the corresponding Fourier transform as $\mathbf{C}(\omega) = \int_{-\infty}^{\infty} \mathrm{d}t e^{\mathrm{i}\omega t} \mathbf{C}(t)$. These correlation tensors, $\mathbf{C} = \{C_{nn'}\}$, have two sets of indices, one for molecules and the other for spatial

https://doi.org/10.1021/acs.jpclett.2c02707
J. Phys. Chem. Lett. 2022, 13, 10943−10951

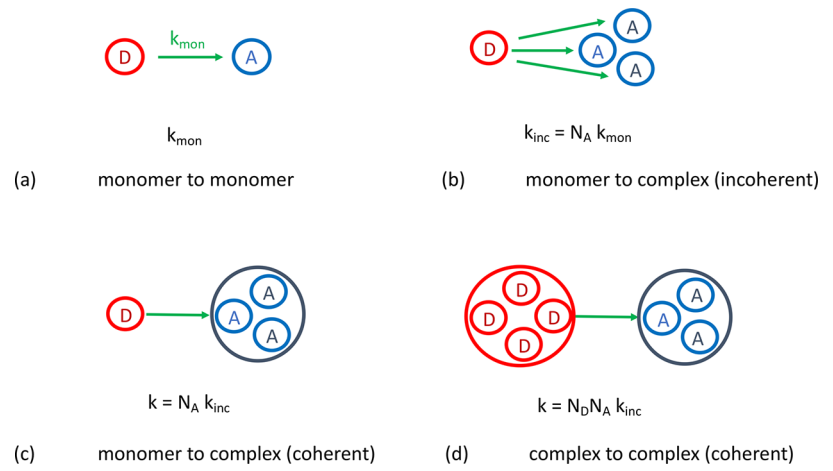

Figure 2. Illustration of various scaling laws of generalized resonant energy transfer (gRET): (a) Incooperative transfer between two monomers is described by k_{mon}. (b) The incoperative transfer rate from a monomer to N_A independent acceptors scales as $k_{inc} = N_A k_{mon}$. (c) The cooperative transfer rate from a monomer to N_A coherently coupled acceptors scales as $k = N_A{}^2 k_{mon} = N_A k_{inc}$. (d) The cooperative transfer rate from N_D coherently coupled donors to N_A coherently coupled acceptors scales as $k = N_D N_A k_{inc}$.

coordinates, so their dimensions are $(3N)^2$. Then, the forward gRET rate is expressed in a compact form as

$$k = \frac{1}{Z_D}\int_{-\infty}^{\infty} dt \mathrm{Tr}[\mathbf{J}^{+}\mathbf{C}_D^{<}(-t)\mathbf{J}\mathbf{C}_A^{>}(t)] = \frac{1}{2\pi Z_D}\int_{-\infty}^{\infty} d\omega \mathrm{Tr}[\mathbf{J}^{+}\mathbf{C}_D^{<}(\omega)\mathbf{J}\mathbf{C}_A^{>}(\omega)] \quad (3)$$

where k is determined by the donor−acceptor coupling $\mathbf{J}$ and the overlap integral of the acceptor's correlation tensor $\mathbf{C}_A^{>}(\omega)$ and the donor's correlation tensor $\mathbf{C}_D^{<}(\omega)$. The general rate expression in eq 3 is illustrated in Figure 1b and is the key result of this Letter. A similar equation can be given for the backward gRET rate.

Basic Properties. In general, when the system is in thermal equilibrium, i.e., $\rho = e^{-\beta H}$, the correlation function obeys the fluctuation−dissipation relationship, $C^{>}(\omega) = \exp(\beta\omega\hbar)\, C^{<}(\omega)$. Applying the relationship to eq 3, we find

$$Z_D k_{D\to A} = Z_A k_{A\to D} \quad (4)$$

which is exactly the detailed balance (DB) condition for gRET. The DB condition can be broken if the donor and acceptor have different temperatures and/or chemical potentials. Then, the net energy flow from the donor to acceptor defines the nonequilibrium steady-state (NESS) flux or current, $F = Z_D k_{D\to A} - Z_A k_{A\to D}$, which has been used previously to define energy transfer pathways in light-harvesting networks[19] as well as in various nonequilibrium transport settings.

In general, the overlap of the dipole correlation tensors in eq 3 is not equivalent to the spectral overlap in FRET. Such a connection can be established only in the far-field, where the donor−acceptor coupling can be taken independently of the molecular index, i.e., $\mathbf{J}_{mn} = \mathcal{J}$. Then, the gRET rate in eq 3 reduces to the standard far-field RET rate

$$k = \frac{2\pi}{Z_D}\int_{-\infty}^{\infty} \mathrm{Tr}[\mathcal{J}^{+}C_{s,D}^{<}(\omega)\mathbf{J}C_{s,A}^{>}(\omega)]d\omega = \frac{2\pi}{Z_D}\mathrm{Tr}(\mathcal{J})^2\int_{-\infty}^{\infty} C_{s,D}^{<}(\omega)C_{s,A}^{>}(\omega)d\omega \quad (5)$$

where the first equality takes the trace in the three-dimensional space and the second equality further assumes an isotropic sample. The spectral correlation function is defined as the sum of all tensor elements

$$C_s(\omega) = \sum_{m,n}[\mathbf{C}]_{mn}(\omega) \quad (6)$$

which represents the absorption or emission part of optical spectra. The double sum in eq 6 reflects the collective effect in the donor or acceptor complex. The influences of the system−bath coupling or the system−cavity coupling on the transfer rate are reflected in the line widths and peak frequencies of these spectral functions, which will be calculated later. However, the relationship between the spectral overlap and transfer rate fails at the near field such as liquids and solvents, so that even the dark states in cavities can participate in energy transfer.[18]

We now examine the effects of spatial coherence (i.e., delocalization) in the donor or acceptor state on the gRET rate. As illustrated in Figure 2, let us consider N-scalings of identical molecules with the same donor−acceptor coupling (i.e., far-field) and without frequency resolution (i.e., assuming a constant spectral overlap). (i) If there is no spatial coherence, then the correlation tensor is diagonal $\mathbf{C} = C_{mon}\,\delta_{mn}$ such that $C_s = NC_{mon}$ and the incohernt transfer rate is $k_{inc} = N_A k_{mon}$ (see Figure 2b). Here, the subscript *mon* refers to the monomer result and *inc* refers to the incoherent rate without any quantum coherence in the donor or acceptor complex. (ii) If the N molecules are fully coherent, then the correlation tensor is constant, $C_{mn} = C_{mon}$, such that $C_s = N^2 C_{mon}$ and the coherence-enhanced transfer rate becomes $k = N_A^2 N_D k_{mon} = N_A N_D k_{inc}$ (see Figure 2c,d). (iii) If the N molecules are partially coherent with coherent size of N_{coh}, then we have $C_s = NN_{coh}C_{mon}$ and $k = N_{A,coh}N_{D,coh}k_{inc}$, which applies for $N > N_{coh}$.

In reality, N_{coh} should be interpreted as the number of coherently coupled molecules, i.e., the localization length, which is limited by dynamic and static disorder in cavity polaritons.[20−22] Taking the example of the exponential correlation, i.e., $C_{mn} = C_{mon}\exp(-|m-n|/N_{coh})$, we can define the effective coherent length

https://doi.org/10.1021/acs.jpclett.2c02707
J. Phys. Chem. Lett. 2022, 13, 10943−10951

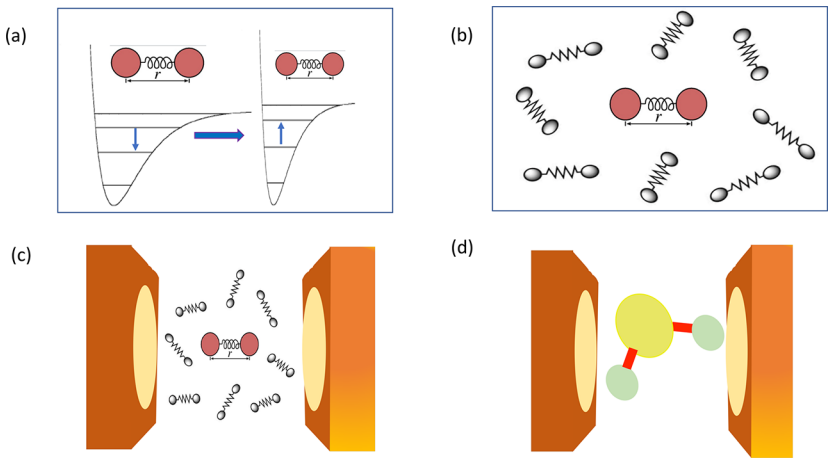

Figure 3. Illustration of various scenarios of resonance vibrational energy transfer (VET): (a) VET from a donor to an acceptor, both modeled as the Morse oscillator; (b) vibrational energy relaxation (VER) due to VET between a central molecule and a distribution of solvent molecules; (c) cavity-assisted VER from a donor molecule to a collection of acceptor molecules coherently coupled by the cavity field; (d) cavity-assisted intramolecular vibrational energy relaxation or redistribution (IVR) resulting from nonlinear coupling between molecular modes in an optical cavity.

$$N_{\text{eff}} = \frac{1}{N}\sum_{n,m}^{N} e^{-|m-n|/N_{\text{coh}}} \approx \frac{1}{N}[(N - N_{\text{coh}})N_{\text{coh}} + N_{\text{coh}}^2 e^{-N/N_{\text{coh}}}] \tag{7}$$

which recovers the large aggregate limit of $N_{\text{eff}} = N_{\text{coh}}$ and the small aggregate limit of $N_{\text{eff}} = N$. Then, the collective transfer rate is given as $k = N_{A,\text{eff}} N_{D,\text{eff}} k_{\text{inc}}$, which interpolates between the spatial coherent and incoherent (i.e., cooperative and incooperative) limits.

The cooperative effects discussed in eq 7 can be simplified for macroscopically homogeneous systems such as solvents or liquids. Here the spatial homogeneity leads to identical coherence between all pairs of molecules, i.e., $C_{ij} = C_{11}\,\delta_{ij} + C_{12}(1 - \delta_{ij})$, where C_{11} is the diagonal tensor element and C_{12} is the off-diagonal tensor element. This holds not only for a homogeneous system, where all donor (or acceptor) molecules are identical, but also for disordered systems, where donor (or acceptor) molecules become equivalent after statistical averaging.[21−23] Let us consider energy relaxation from a single donor to N_A acceptors, as illustrated in Figure 1c. In this case, the gRET rate in eq 3 can be decomposed to

$$\begin{aligned} k &= \frac{1}{2\pi Z_D}\int_{-\infty}^{\infty} N\langle \text{Tr}\mathcal{J}_{DA}\mathcal{J}_{DA}^{+}\rangle C_D^{<}(\omega)C_{A11}^{>}(\omega) \\ &\quad + (N-1)N\langle \text{Tr}\mathcal{J}_{DA1}\mathcal{J}_{DA2}^{+}\rangle C_D^{<}(\omega)C_{A12}^{>}(\omega)\text{d}\omega \\ &= k_{\text{inc}}[1 + (N-1)F] = N_{\text{eff}}k_{\text{inc}} \end{aligned} \tag{8}$$

where $k_{\text{inc}} = N_A k_{\text{mon}}$ and the effective coherence length becomes $N_{\text{eff}} = 1 + (N - 1)\,F$. Here $\langle\cdots\rangle$ represents the configurational average and is given later in eq 14. The enhancement due to quantum coherence is captured by the F factor, defined explicitly as

$$\begin{aligned} F &= \frac{\langle \text{Tr}\mathcal{J}_{DA1}\mathcal{J}_{DA2}^{+}\rangle \int_{-\infty}^{\infty} C_D^{<}(\omega)C_{A12}^{>}(\omega)\text{d}\omega}{\langle \text{Tr}|\mathcal{J}_{DA1}|^2\rangle \int_{-\infty}^{\infty} C_D^{<}(\omega)C_{A11}^{>}(\omega)\text{d}\omega} \\ &\approx \frac{\int_{-\infty}^{\infty} C_D^{<}(\omega)C_{A12}^{>}(\omega)\text{d}\omega}{\int_{-\infty}^{\infty} C_D^{<}(\omega)C_{A11}^{>}(\omega)\text{d}\omega} \end{aligned} \tag{9}$$

the approximation in the second relationship applies only at the far-field. Since the light−matter interaction in optical cavities can be treated homogeneously, the above results apply to gRET in polariton systems.

Equation 3 is general and reduces to the FRET theory in exciton systems as a special case. Specifically, with the electronic transition dipole $\mu \propto (|e\rangle\langle g| + |g\rangle\langle e|)$, we can identify $\mathbf{C}^{>}(\omega) = \mathbf{I}(\omega)$ as the electronic absorption tensor and $\mathbf{C}^{<}(\omega) = \mathbf{E}(\omega)$ as the electronic emission tensor. Then, eq 3 becomes

$$k_{\text{FRET}} = \frac{1}{2\pi}\int_{-\infty}^{\infty} \text{d}\omega \text{Tr}[\mathbf{J}^{\text{T}}\mathbf{E}_D(\omega)\mathbf{J}\mathbf{I}_A(\omega)] \tag{10}$$

which is exactly the generalized-FRET rate for MC systems.[18,24−29] Note the donor−acceptor coupling in FRET is dipolar in nature and can be taken as a real function such that $\mathcal{J}^{+} = \mathcal{J}^{\text{T}}$. We emphasize that the gRET rate formalism presented in this Letter is more general than FRET and is applicable to any resonance quantum transfer processes, including electronic, vibrational, and rotational transitions as well as hybrid transitions via rovibrational resonance, vibronic resonance, polariton resonance, or vibrational-polariton resonance.

Vibrational Coupling. As illustrated in Figure 3, we consider the vibrational interaction potential between two molecules or within a molecule, $U(\vec{R}_1 - \vec{R}_2) = U(\vec{R} - \vec{r}_1 + \vec{r}_2)$, where $\vec{R}$ is the vector connecting the centers of two vibrational coordinates and $\vec{r}_1$ and $\vec{r}_2$ are the vibrational coordinates. Here, the interaction is isotropic so that the potential is central symmetric. Typically, the vibrational amplitude is considerably smaller than the separation, $r \ll R$, such that the Taylor expansion yields

$$\begin{aligned} U(\vec{R}_1 - \vec{R}_2) &= U(R) - \frac{\text{d}U}{\text{d}R}\hat{R}(\vec{r}_1 - \vec{r}_2) \\ &\quad + \frac{1}{2}(\vec{r}_1 - \vec{r}_2)\mathcal{V}_{12}(\vec{r}_1 - \vec{r}_2) + \cdots \end{aligned} \tag{11}$$

where $\hat{R} = \vec{R}/R$ is the unit vector associated with $\vec{R}$. The coupling tensor is defined as

$$\mathcal{V} = R\frac{\text{d}}{\text{d}R}\left(\frac{1}{R}\frac{\text{d}U}{\text{d}R}\right)\hat{R}\cdot\hat{R} + \frac{1}{R}\frac{\text{d}U}{\text{d}R}\mathcal{I}$$

https://doi.org/10.1021/acs.jpclett.2c02707
J. Phys. Chem. Lett. 2022, 13, 10943−10951

where $\mathcal{I}$ is the identity tensor. For the special case of charge interactions, $U(R) \propto 1/R$, the coupling tensor reduces to the standard dipole tensor, i.e., $\mathcal{V} = (3\hat{R}\hat{R} - \mathcal{I})/R^3$. In eq 11, the first-order expansion term does not involve VET and will not be further considered. The second-order expansion term in eq 11 is rewritten as

$$-\vec{r}_1\mathcal{V}_{12}\vec{r}_2 + \frac{1}{2}(\vec{r}_1\mathcal{V}_{12}\vec{r}_1 + \vec{r}_2\mathcal{V}_{12}\vec{r}_2)$$

where the first term describes resonance VET and will be the focus of discussion thereafter. The second term represents a constant contribution of the interaction potential to the site energy and will not be further considered. For compatibility with the gRET formalism, we transform the vibrational coordinate $\vec{r}$ to the linear transition dipole moment μ via $\vec{\mu} = \mu'\vec{r}$, where μ' is the linear coefficient. Then, the donor−acceptor coupling becomes

$$(H_{DA})_{12} = -\vec{r}_1\mathcal{V}_{12}\vec{r}_2 = \vec{\mu}_1\mathcal{J}_{12}\vec{\mu}_2 \tag{12}$$

where $\mathcal{J}_{12} = -\mu_1'\mu_2'\mathcal{V}_{12}$ is the effective dipole coupling tensor.

In gRET, the initial or final state of energy transfer refers to an eigen-state of the donor or acceptor Hamiltonian. In limiting cases, these vibrational eigen-states can be associated with normal or local modes in a molecule. Yet, in general, all vibrational coordinates contribute to the eigen-state nonlinearly, so that we may no longer define a simple collective coordinate in a polyatomic molecule. Further, the donor or acceptor vibrational eigenstate can be defined on different molecules or on the same molecule such that the VET can occur between in the form of VER between molecules (see Figure 3c) or within a molecule in the form of IVR (see Figure 3d), and the gRET formalism presented in this Letter applies to both cases.

As a side note, the vibrational coordinate is generally a nonlinear operator for an anharmonic potential. Taking the example of the Morse potential, we have

$$q = \sqrt{\frac{\hbar}{2m\omega}}[(a + a^+) - \chi(a + a^+)^2 + \cdots]$$

where a and a^+ are the annihilation and creation operators, respectively, and χ denotes the anharmonicity.[30] As a result, the linear excitation can induce not only single-phonon transitions but also multiphonon transitions and dephasing. The latter is also known as anharmonicity-induced dephasing (see Appendix A of ref 31). These nonlinear effects are usually small but can be amplified by the cavity-induced cooperativity.

VET Rate. We apply the gRET theory to vibrational energy transfer (VET) as illustrated for various cases in Figure 3. For monomers (see Figure 3a), the gRET rate formula eq 3 simplifies to eq 5. As an example, we consider the harmonic oscillator potential with frequency ω and dipole operator $\mu = \sqrt{\alpha}(a + a^+)$, where a^- and a^+ are the lowering and raising operators, respectively, and $\alpha = (\mu')^2\hbar/(2m\omega)$ is the coefficient. Assuming slow bath relaxation, we have the Gaussian line-shape[32,33]

$$C_A^>(\omega) = \alpha_A(\nu_A + 1)G(\omega - \omega_A, \lambda_A)$$

$$C_D^<(\omega) = \alpha_D\nu_D G(\omega - \omega_D, \lambda_D)$$

where λ_A (λ_D) is the reorganization energy, ν_A (ν_D) is the vibrational quantum number of the initial state, and ω_A (ω_B) is the vibrational frequency. Here, the Gaussian function is defined as

$$G(\omega, \lambda) = \frac{1}{\sqrt{4\pi\lambda k_B T}}\exp\left(-\frac{\omega^2}{4\lambda k_B T}\right)$$

where $k_B T$ is the thermal energy. Then, the VET rate is given by

$$k = \frac{\mathrm{Tr}\mathcal{J}^2}{2\pi}\alpha_A\alpha_D\nu_D(\nu_A + 1)G(\omega_A - \omega_D, \lambda_A + \lambda_D) \tag{13}$$

which exhibits the maximal transfer rate at the resonance $\omega_A = \omega_D$. The above expressions can be easily extended to the thermal equilibrium by introducing the thermal average, $\langle\nu\rangle = [\exp(\beta\hbar\omega) - 1]^{-1}$, which ensures the DB relation in eq 4. As illustrated in Figure 3b, the VET rate in eq 13 can also describe vibrational energy relaxation (VER) by summing over all acceptors, which results in an ensemble average of molecular configurations. Specifically, the relaxation rate can be obtained by replacing the prefactor in eq 13 with a configurational average:

$$\mathrm{Tr}\mathcal{J}^2 \to \langle\mathrm{Tr}\mathcal{J}^2\rangle = \frac{1}{N_A}\int\rho_A(\vec{R})[\mathrm{Tr}\mathcal{J}^2(\vec{R})]\mathrm{d}\vec{R} \tag{14}$$

where $\rho(\vec{R})$ is the density distribution of acceptor molecules. More generally, we shall also account for orientational distribution in conjunction with the spatial distribution.

To go beyond the monomer case, we now explicitly evaluate eq 3 under the diagonal approximation, previously adopted to approximately evaluate FRET rates in purple bacteria LH_2.[26,33] Specifically, we consider the transfer rate between a pair of delocalized eigenstates, ignoring the correlation between different eigenstates. For simplicity, we limit our discussion to far-field and explicitly evaluate the collective dipole correlation function defined in eq 6 for the jth eigenstate, giving

$$C_j^>(\omega) = S_j\alpha_j(\nu_j + 1)G(\omega - \omega_j, \lambda_j)$$

and a similar expression for $C_j^<(\omega)$. Here, $S_j = \sum_{n,m}c_{n,j}c_{m,j}^*$ is a measure of the coherent size, i.e., $S \approx N_{\mathrm{eff}}$, and $\lambda_j = \sum_n c_{n,j}c_{n,j}^*\lambda_n$ is the effective reorganization energy, where c is the expansion coefficient, defined as $q_n = c_{n,j}q_j$. Using eq 3, we obtain the VET rate from the ith donor state to the jth acceptor state

$$k = \frac{\langle\mathrm{Tr}\mathcal{J}^2\rangle}{2\pi}\alpha_{A,j}\alpha_{D,i}\nu_{D,i}(\nu_{A,j} + 1)S_{A,j}S_{D,i}G(\omega_{A,j} - \omega_{D,i}, \lambda_{A,j} + \lambda_{D,i}) \tag{15}$$

which will be applied to vibrational polaritons below.

Next we turn to cavity-assisted intermolecular VET under vibrational strong coupling (VSC) illustrated in Figure 3c. For simplicity, we consider N identical harmonic oscillators with vibrational frequency ω in a constant optical field with cavity frequency ω_c. The VSC strength is characterized by g for individual oscillators and by $g_N = \sqrt{N}g$ for a collection of N oscillators.[13,34] Then, we obtain the two vibrational polariton frequencies

$$\omega_\pm^2 = \frac{1}{2}(\omega_e^2 + \omega_c^2) \pm \frac{1}{2}\sqrt{(\omega_e^2 - \omega_c^2)^2 + g_N^2\omega_c^4} \tag{16}$$

where the sign corresponds to the two polariton branches and $\omega_e^2 = \omega^2 + g_N^2\omega_c^2$ is the effective oscillator frequency with the account of the dipole self-energy term.[35] The hybrid of the collective molecular and cavity modes is characterized by the mixing angle

$$\tan(\theta) = \frac{g_N\omega_c^2}{\omega_e^2 - \omega_c^2} \tag{17}$$

https://doi.org/10.1021/acs.jpclett.2c02707
J. Phys. Chem. Lett. 2022, 13, 10943−10951

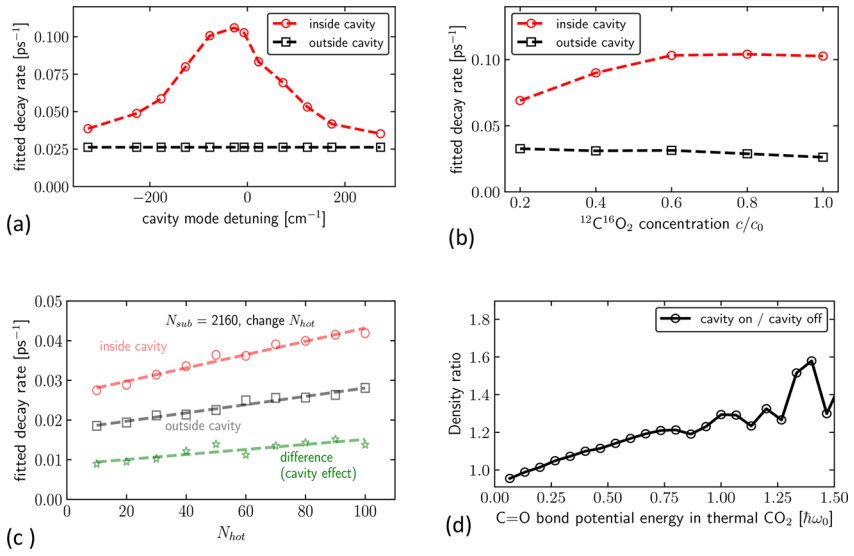

Figure 4. Functional dependences of cavity-assisted VER rate reported in a recent numerical simulation[16] on various control variables: (a) cavity mode detuning; (b) donor molecular concentration; (c) number of hot molecules; (d) energy distribution in the donor. The data and plots in this figure were provided by the authors of the published numerical study.[16]

where the denominator is detuning. The remaining $N-1$ modes are dark states with the unperturbed frequency ω.

As an example, we consider the case where both donor and acceptor are lower vibrational polariton (LP) states. In this case, we have the collective dipole correlation function given as

$$C_-^>(\omega) = N_{-,\mathrm{eff}}\cos^2(\theta/2)\alpha_-^2(\nu_- + 1)G(\omega - \omega_-, \lambda_-)$$

and a similar definition for $C_-^<(\omega)$. Defined in eq 7, N_{eff} reduces to the incoherent monomer limit with $N_{\mathrm{eff}} = 1$ and the fully coherent limit with $N_{\mathrm{eff}} = N$. As a result, the VET rate for the two LP states becomes

$$k = \frac{\langle \mathrm{Tr}\mathcal{J}^2\rangle}{2\pi}\alpha_{A-}\alpha_{D-}\nu_{D-}(\nu_{A-} + 1)N_{A-,\mathrm{eff}}N_{D-,\mathrm{eff}}\cos^2(\theta_A/2)$$
$$\cos^2(\theta_D/2)G(\omega_{A-} - \omega_{D-}, \lambda_{A-} + \lambda_{D-}) \quad (18)$$

where the reorganization energy is rescaled according to $\lambda_- = \lambda\cos^2(\theta/2)/N$. Similar results can be obtained for other pairs of polaritons or molecular states. For molecules outside of the cavity or far off-resonant with the cavity frequency, we can set $\cos^2(\theta/2) = 1$.

Cavity-Assisted VET: A Case Study. A recent numerical study by Li, Nitzan, and Subnotik[16] explores collective VSC effects on VER of a small fraction of hot molecules in the CO_2 solvent. In their simulation, the excess vibrational energy of the hot molecules is transferred transiently to the coherent lower polariton state (LP) and subsequently dissipates to dark states or solvent molecules, thus leading to an acceleration of VER of the hot molecules. Since the second step is almost irreversible, we will focus on the VET process as illustrated in Figure 2c.

Several intriguing phenomena have been observed in the simulation and can be understood based on the VET rate in eq 18:

1. Equation 18 depends on the frequency detuning via the spectral overlap (i.e., the Gaussian line shape function) and the projection of the polaritons to the molecular basis (i.e., the prefactor), thus reproducing the bell shape in Figure 4a (i.e., Figure 3 of the original paper) of the reported simulation. Further, the LP wave function yields the ratio of $\sin^2(\theta/2)$ and $\cos^2(\theta/2)/N$ between the photonic energy and molecular energy, so that the transferred energy to the cavity photon is higher than to molecules, in agreement with Figure 2c,d of ref 16. The thermalization process will eventually recover the energy equipartition for the cavity photons and molecules in the long-time limit, as ensured by the DB condition in eq 4.
2. The Rabi frequency depends on the solvent concentration as $g_N = \sqrt{N}g$ and leads to the concentration-dependence in the peak frequency (see Figure 4a of the referred simulation). According to eq 7, the VER rate at the far field is proportional to the spectra overlap, which increases with the LP frequency shift. Thus, the cavity-enhanced VER rate increases with the solvent concentration, consistent with Figure 4b (i.e., Figure 4b of the reported simulation).
3. The hot molecules (i.e., donors) can be coherently coupled via the cavity field or the intermolecular interaction. Then the VER rate in eq 7 is proportional to the emission intensity, which in turn is proportional to N, i.e., the number of coherently coupled hot molecules, thus explaining the N-dependence in Figure 4c (i.e., Figure 5 of the referred simulation).
4. Since the O−C bond is modeled as a Morse potential, its average frequency decreases with the vibrational energy. Then, the hot donor molecule is in better resonance with the higher vibrational excited states of the acceptor molecule, so the energy is transferred to the low-energy tail of the acceptor state distribution as shown in Figure 4d (i.e., Figure 7b of the reported simulation).

Discussion. The proposed theory is motivated by two sets of cavity experiments in the VSC regime: (i) cavity-assisted intermolecular vibrational energy relaxation (VER) or intramolecular vibrational energy relaxation or redistribution (IVR)[10−12] and (ii) cavity-catalyzed ground-state chemical reactions.[6−9] The gRET rate expression in this Letter applies directly to the first set of experiments and related numerical studies. In comparison, the second set of experiments on cavity-catalyzed reactions involve thermal activation and are not

https://doi.org/10.1021/acs.jpclett.2c02707
J. Phys. Chem. Lett. 2022, 13, 10943−10951

directly described within the framework of gRET. However, both in solvents and in optical cavities, vibrational energy transfer, relaxation. and redistribution are responsible for thermalization and thermal fluctuations of reactive systems and thus can play a potentially important role in cavity-catalyzed reactions.

Specifically, it is revealing to analyze the intriguing phenomena of cavity-catalyzed adiabatic chemical reactions in the context of enhanced VER, as suggested by the authors.[16] In the current context, the cavity-induced enhancement of the vibrational relaxation rate of the solute molecule results in an increase in the effective friction coefficient

$$\eta_{\mathrm{VSC}} = \eta N_{\mathrm{eff}} \tag{19}$$

where N_{eff} is the effective coherent number defined in eq 7. According to the Kramers rate theory,[36,37] the N_{eff}-fold increase in the friction constant leads to the enhanced reaction rate in the energy diffusion regime as $k_r \propto \eta_{\mathrm{VSC}}$ and the suppressed rate in the spatial diffusion regime as $k_r \propto 1/\eta_{\mathrm{VSC}}$. The gRET theory presented here connects the reaction rate to the polariton spectral line-shape and molecular density, in agreement with experiments. Yet, the kinetic effect arising from enhanced effective friction is largely temperature-independent, takes different functional forms in the under-damped and over-damped regimes, and cannot explain the orders of magnitude of change induced by cavities.[38,39] Thus, VSC-catalyzed reactions require further analysis,[40−44] which likely involves a quantum rate calculation[35], and possibly a different mechanism.

In fact, a recent quantum transition state theory (TST) analysis[35] attributes the VSC modification of reaction rates to vibrational frequency shifts in the reactive well and transition-state barrier. The reported perturbation analysis of vibrational polariton modes[35] predicts the dependences on temperature, cavity frequency, and light−matter coupling strength. However, the collective effect cannot be easily explained by incoherent thermal activation within the TST framework. In this sense, the thermal rate calculation proposed for VSC-catalyzed reactions and the gRET theory developed for VSC-assisted vibrational dynamics are complementary and can be integrated to yield a more complete picture. Of particular relevance is the potential application of gRET to intramolecular vibrational energy redistribution (IVR) in cavities, as exemplified by the solvated ABA model illustrated in Figure 2d, which has been suggested as a mechanism to understand cavity-catalyzed reactions.[45,46]

Finally, we comment on the validity of classical simulations of quantum dynamics. The quantum correlation function has a simple classical limit, which can be supplemented with quantum correlations to ensure DB.[31,47,48] In fact, the spectrum of the harmonic potential or the Morse potential can be described accurately by classical dynamics,[30] within the framework of quantum−classical correspondence.[49−52] Yet, classical simulations may fail to capture more subtle quantum effects. An interesting example is the system−bath entanglement in the generalized FRET rate in eq 10. In an MC system, the initial state of the donor's emission $E(\omega)$ is an entangled equilibrium state of system and bath and cannot be factorized. This nonfactorized initial state brings technical difficulties in computing the emission spectrum and FRET rate in MC systems and has been a subject of recent studies.[18,53,54]

Summary. The generalized resonant energy transfer (gRET) theory encompasses various degrees of freedom as well as coherently coupled composite states and reduces to the FRET or MC-FRET rate in the special case of excitation energy transfer. The resulting rate expression in eq 3 allows us to establish the basic properties of gRET: (i) The rate obeys the DB condition in eq 4 when the donor and acceptor are at the same temperature and can lead to a NESS flux when at different temperatures. (ii) The gRET rate is proportional to the overlap between the donor's correlation tensor $C_D^<$ and acceptor's correlation tensor $C_A^>$, which is not equivalent to the spectral overlap except in the far-field limit. (iii) The collective spectral function and rate have simple scalings with the effective coherent size defined in eq 7, which equals the number of molecules for small aggregates but becomes the coherent size for large aggregates. (iv) The collective rate in homogeneous systems such as solvents or liquids can be decomposed to the monomer and coherence contributions as in eq 8, and the ratio of the two contributions defines the quantum enhancement factor in eq 9. (v) The donor−acceptor coupling tensor $\mathcal{J}$ can be determined from the interaction potential as in eq 12, thus specifying its orientational and spatial dependences.

The application of gRET to cavity-assisted VER provides a physical explanation of intriguing phenomena including cooperativity, resonance, and anharmonicity, as shown in a recent simulation.[16] Though demonstrated in cavity-assisted intermolecular VER, the gRET formalism can apply equally well to intramolecular vibrational energy relaxation or redistribution (IVR) in cavities, as exemplified by the solvated ABA model illustrated in Figure 2d.[45,46] The correlated vibrational mode coupling in polyatomic molecules may shed light on the VSC-induced phenomena in energy transfer and reaction kinetics and is an interesting subject for further study.

■ ASSOCIATED CONTENT

Supporting Information

The Supporting Information is available free of charge at https://pubs.acs.org/doi/10.1021/acs.jpclett.2c02707.

Derivation and detailed balance of gRET rate; VSC model and vibrational polaritons (PDF)

■ AUTHOR INFORMATION

Corresponding Author

Jianshu Cao − *Department of Chemistry, Massachusetts Institute of Technology, Cambridge, Massachusetts 02139, United States;* Present Address: Freiburg Institute for Advanced Studies (FRIAS), University of Freiburg, 79104, Freiburg, Germany; orcid.org/0000-0001-7616-7809; Email: jianshu@mit.edu

Complete contact information is available at: https://pubs.acs.org/10.1021/acs.jpclett.2c02707

Notes

The author declares no competing financial interest.

■ ACKNOWLEDGMENTS

This work is supported by NSF (CHE 1800301 and CHE 1836913) and MIT Sloan Fund. The author thanks the authors of the recent numerical study[16] for the data and plots used in Figure 4, of this Letter. The author also acknowledges the sponsorhsip of the Rosi and Max Varon Visiting Professorship at the Weizmann Institute of Science and the support of Maria Curie FRIAS COFUND Fellowship Programme (FCFP) during his sabbatical. The research leading to these results has received funding from the European Union's Horizon 2020 research and

innovation programme under the Marie Sktodowska-Curie grant agreement No 754340. An early version of this Letter was posted on arXiv (2201.12117) on Jan. 27, 2022.

REFERENCES

(1) Förster, T. In *Modern Quantum Chemistry. Istanbul Lectures. Part III: Action of Light and Organic Crystals*; Sinanoglu, O., Ed.; Academic Press: New York, 1965; Vol. 3; pp 93−137.
(2) May, V.; Kühn, O.*Charge and energy transfer dynamics in molecular systems*; AIP Publishing.
(3) Cao, J.; Cogdell, R. J.; Coker, D. F.; Duan, H.-G.; Hauer, J.; Kleinekathöfer, U.; Jansen, T. L. C.; Mančal, T.; Miller, R. J. D.; Ogilvie, J. P.; et al. Quantum Biology Revisited. *Science Advances* **2020**, *6*, eaaz4888.
(4) Baiz, C. R.; Blasiak, B.; Bredenbeck, J.; Cho, M.; Choi, J.-H.; Corcelli, S. A.; Dijkstra, A. G.; Feng, C.-J.; Garrett-Roe, S.; Ge, N.-H.; et al. Vibrational spectroscopic map, vibrational spectroscopy, and intermolecular interaction. *Chem. Rev.* **2020**, *120* (15), 7152−7218.
(5) Bigwood, R.; Gruebele, M.; Leitner, D. M.; Wolynes, P. G. The vibrational energy flow transition in organic molecules: Theory meets experiment. *Proc. Natl. Acad. Sci. U. S. A.* **1998**, *95* (11), 5960−5964.
(6) Garcia-Vidal, F. J.; Ciuti, C.; Ebbesen, T. W. Manipulating matter by strong coupling to vacuum fields. *Science* **2021**, *373*, 6551.
(7) Thomas, A.; George, J.; Shalabney, A.; Dryzhakov, M.; Varma, S. J.; Moran, J.; Chervy, T.; Zhong, X.; Devaux, E.; Genet, C.; et al. Ground-state chemical reactivity under vibrational coupling to the vacuum electromagnetic field. *Angew. Chem.* **2016**, *128*, 11634−11638.
(8) Lather, J.; Bhatt, P.; Thomas, A.; Ebbesen, T. W.; George, J. Cavity catalysis by cooperative vibrational strong coupling of reactant and solvent molecules. *Angew. Chem., Int. Ed.* **2019**, *58*, 10635.
(9) Hirai, K.; Hutchison, J. A.; Uji-i, H. Recent progress of vibropolaritonic chemistry. *ChemPlusChem.* **2020**, *85*, 1981−1988.
(10) Dunkelberger, A. D.; Spann, B. T.; Fears, K. P.; Simpkins, B. S.; Owrutsky, J. C. Modified relaxation dynamics and coherent energy exchange in coupled vibration-cavity polaritons. *Nat. Commun.* **2016**, *7*, 13504.
(11) Xiang, B.; Ribeiro, R. F.; Dunkelberger, A. D.; Wang, J.; Li, Y.; Simpkins, B. S.; Owrutsky, J. C.; Yuen-Zhou, J.; Xiong, W. Two-dimensional infrared spectroscopy of vibrational polaritons. *Proc. Natl. Acad. Sci. U.S.A.* **2018**, *115*, 4845.
(12) Xiang, B.; Ribeiro, R. F.; Du, M.; Chen, L.; Yang, Z.; Wang, J.; Yuen-Zhou, J.; Xiong, W. Intermolecular vibrational energy transfer enabled by microcavity strong light-matter coupling. *Science* **2020**, *368*, 665−667.
(13) Flick, J.; Ruggenthaler, M.; Appel, H.; Rubio, A. Atoms and molecules in cavities, from weak to strong coupling in quantum-electrodynamics (qed) chemistry. *Proc. Natl. Acad. Sci. U. S. A.* **2017**, *114*, 3026−3034.
(14) Schäfer, C.; Flick, J.; Ronca, E.; Narang, P.; Rubio, A. Shining Light on the Microscopic Resonant Mechanism Responsible for Cavity-Mediated Chemical Reactivity. *arXiv* **2021**, 2104.12429.
(15) Li, T. E.; Subotnik, J. E.; Nitzan, A. Cavity molecular dynamics simulations of liquid water under vibrational ultrastrong coupling. *Proc. Natl. Acad. Sci. U.S.A.* **2020**, *117*, 18324−18331.
(16) Li, T. E.; Nitzan, A.; Subotnik, J. E. Collective Vibrational Strong Coupling Effects on Molecular Vibrational Relaxation and Energy Transfer: Numerical Insights via Cavity Molecular Dynamics Simulations. *Angew. Chem.* **2021**, *60*, 15533−15540.
(17) Du, M.; Ribeiro, R. F.; Yuen-Zhou, J. Remote control of chemistry in optical cavities. *Chem.* **2019**, *5*, 1167−1181.
(18) Ma, J.; Cao, J. Forster resonance energy transfer, absorption and emission spectra in multichromophoric systems. I. Full cumulant expansions and system-bath entanglement. *J. Chem. Phys.* **2015**, *142*, 094106.
(19) Yang, P.-Y.; Cao, J. Steady-State Analysis of Light-harvesting Energy Transfer Driven by Incoherent Light: From Dimers to Networks. *J. Phys. Chem. Lett.* **2020**, *11*, 7204−7211.
(20) Wersäll, M.; Munkhbat, B.; Baranov, D.; Herrera, F.; Cao, J.; Antosiewicz, T. J.; Shegai, T. Correlative Dark-Field and Photoluminescence Spectroscopy of Individual Plasmon-Molecule Hybrid Nanostructures in a Strong Coupling Regime. *ACS Photonics* **2019**, *6*, 2570−2576.
(21) Engelhardt, G.; Cao, J. Unusual Dynamical Properties of Disordered Polaritons in Micocavities. *Phys. Rev. B* **2022**, *105*, 064205.
(22) Engelhardt, G.; Cao, J. Polarition localization and spectroscopic properties of disordered quantum emitters in spatially-extended microcavities. *arXiv* **2022**, 2209.02909.
(23) Cederbaum, L. S. Cooperative molecular structure in polaritonic and dark states. *J. Chem. Phys.* **2022**, *156*, 184102.
(24) Sumi, H. Theory on Rates of Excitation-Energy Transfer between Molecular Aggregates through Distributed Transition Dipoles with Application to the Antenna System in Bacterial Photosynthesis. *J. Phys. Chem. B* **1999**, *103*, 252.
(25) Scholes, G. D.; Fleming, G. R. On the Mechanism of Light Harvesting in Photosynthetic Purple Bacteria: B800 to B850 Energy Transfer. *J. Phys. Chem. B* **2000**, *104*, 1854.
(26) Hu, X.; Ritz, T.; Damjanovic, A.; Autenrieth, F.; Schulten, K. Photosynthetic apparatus of purple bacteria. *Q. Rev. Biophys.* **2002**, *35*, 1.
(27) Jang, S.; Newton, M. D.; Silbey, R. J. Multichromophoric Foerster Resonance Energy Transfer. *Phys. Rev. Lett.* **2004**, *92*, 218301.
(28) Moix, J.; Ma, J.; Cao, J. Forster resonance energy transfer, absorption and emission spectra in multichromophoric systems. III. Exact stochastic path integral evaluation. *J. Chem. Phys.* **2015**, *142*, 094108.
(29) Wang, S.; Chuang, Y.-T.; Hsu, L.-Y. Macroscopic quantum electrodynamics approach to multichromophoric excitation energy transfer. I. Formalism. *J. Chem. Phys.* **2022**, *157*, 184107.
(30) Wu, J.; Cao, J. Linear and nonlinear response functions of a Morse oscillator: Classical divergence and the uncertainly principle. *J. Chem. Phys.* **2001**, *115*, 5381.
(31) Yang, S.; Shao, J.; Cao, J. Nonperturbative vibrational energy relaxation effects on vibrational line-shapes. *J. Chem. Phys.* **2004**, *121*, 11250.
(32) Mukamel, S.*Principles of nonlinear optical spectroscopy*; Oxford University Press on Demand, 1999.
(33) Cleary, L.; Cao, J. Optimal thermal bath for robust excitation energy transfer in disordered light-harvesting complex 2 of purple bacteria. *New J. Phys.* **2013**, *15*, 125030.
(34) Power, E. A.; Zienau, S. Coulomb gauge in non-relativistic quantum electro-dynamics and the shape of spectral lines. *Philos. Trans. R. Soc. London A* **1959**, *251*, 427.
(35) Yang, P.-Y.; Cao, J. Quantum Effects in Chemical Reactions under Polaritonic Vibrational Strong Coupling. *J. Phys. Chem. Lett.* **2021**, *12*, 9531.
(36) Pollak, E.; Grabert, H.; Hänggi, P. Theory of activated rate processes for arbitrary frequency dependent friction: Solution of the turnover problem. *J. Chem. Phys.* **1989**, *91* (7), 4073−4087.
(37) Nitzan, A.*Chemical Dynamics in Condensed Phases: Relaxation, Transfer and Reactions in Condensed Molecular Systems*; Oxford University Press: Oxford, U.K., 2007.
(38) Mandal, A.; Li, X.; Huo, P. Theory of vibrational polariton chemistry in the collective coupling regime. *J. Chem. Phys.* **2022**, *156*, 014101.
(39) Lindoy, L. P.; Mandal, A.; Reichman, D. R. Resonant Cavity Modification of Ground State Chemical Kinetics. *J. Phys. Chem. Lett.* **2022**, *13*, 6580−6586.
(40) Galego, J.; Climent, C.; Garcia-Vidal, F. J.; Feist, J. Cavity Casimir-Polder Forces and Their Effects in Ground-State Chemical Reactivity. *Phys. Rev. X* **2019**, *9*, 021057.
(41) Li, T. E.; Nitzan, A.; Subotnik, J. E. On the origin of ground-state vacuum-field catalysis: Equilibrium consideration. *J. Chem. Phys.* **2020**, *152*, 234107.
(42) Campos-Gonzalez-Angulo, J. A.; Yuen-Zhou, J. Polaritonic normal modes in transition state theory. *J. Chem. Phys.* **2020**, *152*, 161101.

https://doi.org/10.1021/acs.jpclett.2c02707
J. Phys. Chem. Lett. 2022, 13, 10943−10951

(43) Triana, J.; Herrera, F. Self-dissociation of polar molecules in a confined infrared vacuum. *ChemRxiv* **2020**.
(44) Fischer, E. W.; Anders, J.; Saalfrank, P. Cavity-Altered Thermal Isomerization Rates and Dynamical Resonant Localization in Vibropolaritonic Chemistry. *arXiv* **2022**, 2109.13574.
(45) Wang, D. S.; Neuman, T.; Yelin, S. F.; Flick, J. Cavity-modified unimolecular dissociation reactions via intramolecular vibrational energy redistribution. *arXiv* **2022**, 2109.06631.
(46) Kryvohuz, M.; Cao, J. Noise-induced dynamics symmetry breaking and stochastic transitions in ABA molecules: I. Classification of vibrational modes. *J. Phys. Chem. B* **2010**, *114*, 6549.
(47) Egorov, S. A.; Everitt, K. F.; Skinner, J. L. Quantum dynamics and vibrational relaxation. *J. Phys. Chem. A* **1999**, *103* (47), 9494−9499.
(48) Shi, Q.; Geva, E. Vibrational energy relaxation in liquid oxygen from a semiclassical molecular dynamics simulation. *J. Phys. Chem. A* **2003**, *107*, 9070.
(49) Kryvohuz, M.; Cao, J. Quantum-classical correspondence in response theory. *Phys. Rev. Lett.* **2005**, *95*, 180405.
(50) Kryvohuz, M.; Cao, J. Classical divergence of nonliner response functions. *Phys. Rev. Lett.* **2006**, *96*, 030403.
(51) Gruenbaum, S. M.; Loring, R. F. Interference and quantization in semiclassical response functions. *J. Chem. Phys.* **2008**, *128*, 124106.
(52) Loring, R. F. Mean-trajectory approximation for electronic and vibrational-electronic nonlinear spectroscopy. *J. Chem. Phys.* **2017**, *146*, 144106.
(53) Ma, J.; Moix, J.; Cao, J. Forster resonance energy transfer, absorption and emission spectra in multichromophoric systems. II. Hybrid cumulant expansion. *J. Chem. Phys.* **2015**, *142*, 094107.
(54) Chenu, A.; Cao, J. Construction of multichromophoric spectra from monomer data: Applications to resonant energy transfer. *Phys. Rev. Lett.* **2017**, *118*, 013001.

https://doi.org/10.1021/acs.jpclett.2c02707
J. Phys. Chem. Lett. 2022, 13, 10943−10951